Final-state symmetry of Na 1*s* core-shell excitons in NaCl and NaF

K. P. Nagle,[1] G. T. Seidler,[1,*] E. L. Shirley,[2] T. T. Fister,[1,3] J. A. Bradley,[1] and F. C. Brown[1]
[1]*Department of Physics, University of Washington, Seattle, Washington 98105, USA*
[2]*Optical Technology Division, NIST, Gaithersburg, Maryland 20899-8441, USA*
[3]*Materials Science Division, Argonne National Laboratory, Argonne, Illinois 60439, USA*
(Received 27 February 2009; revised manuscript received 26 May 2009; published 8 July 2009)

We report measurements of the Na 1*s* contribution to the nonresonant inelastic x-ray scattering (NRIXS) from NaCl and NaF. Prior x-ray absorption studies have observed two pre-edge excitons in both materials. The momentum-transfer dependence (q dependence) of the measured NRIXS cross section and of real-space full multiple scattering and Bethe-Salpeter calculations determine that the higher-energy core excitons are *s* type for each material. The lower-energy core excitons contribute at most weakly to the NRIXS signal and we propose that these may be surface core excitons, as have been observed in several other alkali halides. The analysis of the orbital angular momentum of these features leads to a discussion of the limited sensitivity of NRIXS measurements to *d*-type final states when investigating 1*s* initial states. In this case the *s*- and *p*-type final density of states can be characterized by measurements at a small number of momentum transfers. This is in contrast to the case of more complex initial states for which measurements at a large number of momentum transfers are needed to separate the rich admixture of accessible and contributing final-state symmetries.

DOI: 10.1103/PhysRevB.80.045105 PACS number(s): 71.35.−y, 78.70.Ck, 71.20.Ps, 61.05.cj

I. INTRODUCTION

The interaction between the photoelectron and the concomitant hole which is present in electronic excited-state spectroscopies plays an important role in the optical and electronic properties of both condensed and molecular phases.[1–4] This interaction is responsible for so-called final-state effects, wherein the photoelectron wave function in the excited state does not correspond to an unoccupied state for the ground state of the system; the interaction with the core hole results in a fundamental modification of the density of states (DOS). The prototypical case in point is the formation of core-hole excitons, as is frequently observed in x-ray absorption spectroscopy (XAS) and related experimental methods.[2–5] Recent progress in both real-space and reciprocal-space treatments of XAS incorporates the interaction between the photoelectron and core hole to account for final-state effects, resulting in significant improvements in calculations of XAS in the near-edge region.[1,6–11]

Measurements of nonresonant x-ray Raman scattering (XRS), the core-shell contribution to nonresonant inelastic x-ray scattering (NRIXS), are blossoming as an alternative to and extension of XAS. In the limit of low momentum transfer (q), XRS provides a bulk-sensitive measurement whose transition matrix element is closely related to that for the absorption coefficient in XAS.[9,12–16] However, as q increases, XRS becomes sensitive to dipole-forbidden final states, thus allowing a more complete investigation of the spectrum of possible excited states.[2,17] XRS measurements have been used to determine the orbital angular momentum of excitons and other resonances in several materials.[2,3,18–21]

Here, we report new XRS measurements of the q dependence of excitonic features associated with the Na 1*s* initial states of NaCl and NaF. The optical and electronic properties of alkali halides have seen several decades of work and they serve as important test cases for understanding final-state effects in insulators. Most relevant for the present paper, there have been recent XAS and resonant Auger studies of the Na 1*s* initial state in both compounds which found demonstrably excitonic pre-edge features.[22,23] While it has been difficult to explain the origin of two dipole-forbidden excitons in NaF,[23] there is good reason to believe that all of the observed pre-edge features are dipole forbidden for XAS from the Na 1*s* initial state.[22,23] Their weak presence in the XAS measurements (where they should nominally be absent because of the dipole selection rule) is made possible by the symmetry-breaking effects of vibrational disorder.[24]

Our q-dependent XRS measurements directly demonstrate that the underlying DOS in the pre-edge region is indeed predominantly dipole forbidden and new real-space full multiple scattering (RSFMS) and Bethe-Salpeter equation (BSE) calculations identify the DOS as being overwhelmingly *s* type. However, the XRS spectra find that this DOS is associated with the higher-energy pre-edge feature in NaCl and most clearly in NaF with little or no signal from the lower-energy features. We discuss possible explanations for this behavior, including the small probability of $1s \rightarrow \varepsilon d$ transitions even at high-momentum transfer and the weakness of spin-flip scattering in XRS, but are unable to find a model for two bulk excitons for the Na 1*s* initial state which is consistent with both theory and experiment. Given the experimental details of the prior XAS measurements, we propose that the lower-energy excitons in both materials may be surface core excitons, as have been observed in several other alkali halides. Further measurements will be necessary to test this hypothesis.

II. THEORY

A. Nonresonant inelastic x-ray scattering

The double-differential cross section for NRIXS is

 ©2009 The American Physical Society

$$\frac{d^2\sigma}{d\Omega d\omega} = \left(\frac{d\sigma}{d\omega}\right)_{\mathrm{Th}} S(\mathbf{q},\omega), \tag{1}$$

where $(d\sigma/d\omega)_{\mathrm{Th}}$ is the Thomson cross section, $\mathbf{q}$ is the momentum transfer from the incident photon to the system, and $\hbar\omega$ is the energy loss of the incident photon. The dynamic structure factor

$$S(\mathbf{q},\omega) = \sum_f |\langle f|e^{i\mathbf{q}\cdot\mathbf{r}}|i\rangle|^2 \delta(E_f - E_i - \hbar\omega), \tag{2}$$

where i and f label the initial and final states and there is an implicit sum over all electrons. The contribution of the valence electrons to $S(\mathbf{q},\omega)$ is typically called Compton or valence Compton scattering, whereas the contribution from core electrons is most often called nonresonant XRS.

In the dipole limit $qa \ll 1$, where a is the average radius of the photoelectron's initial state, the XRS contribution to $S(\mathbf{q},\omega)$ becomes proportional to the usual x-ray absorption coefficient $\mu(\hat{\varepsilon},E_1)$ but with correspondence between the direction of $\mathbf{q}$ and the polarization direction $\hat{\varepsilon}$ and between the XRS energy loss $\hbar\omega$ and the XAS incident photon energy E_1.[9,12–16] Note that the incident photon energy in XRS measurements is much larger than the energy loss and consequently XRS provides a bulk-sensitive alternative to many traditional soft x-ray measurements of XAS.[13,25] The strong penetration of the incident radiation uniquely allows for compatibility with extreme environments[26] such as high-pressure cells, which has lately led to several interesting results.[14,16,27,28]

At higher momentum transfer, however, nondipole transition channels become important and XRS measurements can provide a more complete characterization of the full spectrum of final states for electronic excitations.[2,17] Theoretical methods for XAS calculation have recently been extended to full calculations of the q dependence of $S(q,\omega)$,[9,11,29] and the advent of the third-generation light sources together with improved XRS spectrometers has enabled a rapid growth of applications of q-dependent XRS.[3,15,16,18,19,21,28,30–32] For polycrystalline materials, such as those investigated in this work, the core-electron contribution to $S(q,\omega)$ can be decomposed into a sum of contributions from final states with particular orbital angular momentum l,

$$S(q,\omega) = \sum_l S_l(q,\omega) = \sum_l (2l+1)|M_l(q,\omega)|^2 \rho_l(\omega), \tag{3}$$

where $\rho_l(\omega)$ are the angular momentum-projected local final density of states or l DOS.

$$|M_l(q,\omega)|^2 = (2l_i+1)\sum_{l'}(2l'+1) \times \left|\begin{pmatrix} l_i & l' & l \\ 0 & 0 & 0 \end{pmatrix} \int dr r^2 R_l(r,\omega) j_{l'}(qr) R_{l_i}(r)\right|^2, \tag{4}$$

where l_i and l are the initial and final angular momentum quantum numbers, are essentially atomic weighting factors.[9,33] Given that the $|M_l(q,\omega)|^2$ coefficients may be calculated reliably, Eq. (3) provides two complementary approaches. First, when $S(q,\omega)$ is measured over a sufficiently wide range of q,[34] the system of linear equations in Eq. (3) may be inverted to provide a direct, experimental measurement of $\rho_l(\omega)$.[2,18–21] Second and conversely, Eq. (3) serves as the foundation to determine $S(q,\omega)$ from a theoretical calculation of $\rho_l(\omega)$.[9]

B. Real-space full multiple-scattering calculations

l-DOS calculations were performed using a q-dependent extension of the FEFF8.2 RSFMS software package.[9,35] This code uses a single-particle Green's function employing self-consistent muffin-tin potentials. Potentials are calculated for three distinguishable atoms: the central scattering Na atom, the other Na atoms, and the Cl atoms. Both the self-consistent potentials and the final $S(q,\omega)$ are converged with respect to the number of angular momenta in the basis and the number of atoms included in the calculation. The calculations use the default statically screened core hole and Hedin-Lundquist self-energy. For both NaCl and NaF, convergence occurs for $l=3$ and clusters of 69 atoms. To aid convergence, the source atom was displaced one interatomic spacing from the center of the cluster.

C. Bethe-Salpeter calculations

We also carried out calculations of the imaginary part of the dielectric function, $\varepsilon_2(\mathbf{q},\omega)$, with the framework of solution of the electron-core hole Bethe-Salpeter equation. From $\varepsilon_2(\mathbf{q},\omega)$, one can obtain other quantities, e.g., $S(\mathbf{q},\omega)$, generalized oscillator strength (GOS) and l DOS. This was done following an approach described earlier.[7,32] An effective two-particle, electron-core hole equation of motion was solved, wherein the electron and hole were dressed by one-particle self-energies comparable to those used in earlier work[10] and interacted through the above screened interaction. In this way, several many-body effects were included in the calculation. We used a real-space method to calculate screening of the electron-core hole interaction. This approach is based on a combination of atomic-structure calculations and solid-state calculations done within the random-phase approximation and use of a model-dielectric function to ensure the correct long-range boundary conditions.[8] Additional Lorentzian broadening with 2 eV full width at half maximum was included to facilitate comparison to measured spectra and accompanying spectral resolution. Exploiting the octahedral Na^+-site symmetry, we averaged over the momentum-transfer direction (or sample orientation direction) using momentum transfers of the form

$$\frac{q_x}{q} = \left[\frac{1}{3} + \frac{2}{15}\sqrt{10}\right]^{1/2},$$

$$\frac{q_y}{q} = \frac{q_z}{q} = \left[\frac{1}{3} - \frac{1}{15}\sqrt{10}\right]^{1/2}. \tag{5}$$

This achieves correct averaging over anisotropy resulting from the difference between $3d$-derived e_g and t_{2g} contributions to Na $1s$ excited-state spectra, whereas $3s$- and $3p$-derived contributions are automatically isotropic.[36]

III. EXPERIMENT

We performed NRIXS measurements with the lower-energy resolution inelastic x-ray (LERIX) scattering user facility[37] at the undulator beamline 20-ID of the Advanced Photon Source at Argonne National Laboratory. Using LERIX, NRIXS spectra can be acquired simultaneously by up to nineteen independent analyzer-detector pairs, resulting in relatively high throughput of measurements despite the small NRIXS cross section. Working at the Si (555) reflection of the LERIX analyzers, the analyzer energy is fixed at 9890 eV. The binding energy of an electron in the Na 1*s* orbital in elemental Na is 1072 eV; therefore, the incident photon energy was scanned through an energy range near 10962 eV.

Powder samples of NaCl and NaF (Alfa-Aesar, 99.99% purity) were pressed into pellets. A large, flat face of the pellet was oriented in a reflection geometry at about 20° elevation with respect to the horizontal (i.e., the beam direction). As a result, the four lowest-q LERIX analyzers were at least partially blocked by strong absorption from the sample. Furthermore, data from one of the higher-q analyzers was removed due to problems with preamplifier noise. For an incident photon energy of 10962 eV, the remaining fourteen detectors have q=4.3, 5.0, 5.8, 6.5, 7.2, 8.4, 9.0, 9.5, 9.9, 10.3, 10.6, 10.8, 11.0, and 11.1 Å^{-1}. Each pellet had a thickness of several times the penetration length of the material at typical incident photon energies (153 μm for NaCl and 450 μm for NaF at 10962 eV). The overall energy resolution of 1.4 eV was mainly monochromator limited. Self-consistency between energy losses within individual spectra is better than 0.1 eV (Ref. 37); however, the overall energy-loss scale may have ~1 eV systematic error due to malfunction of the monochromator encoder. Consequently, the spectra for both compounds were shifted to ~0.5 eV higher energy loss so as to agree with the energy calibration of recent XAS studies.[22,23] All measurements took place at room temperature in a He-gas environment.

A total of 352 and 8 s integration time per point are used in the near-edge and extended region, respectively, for NaCl. A total of 256 and 8 s integration time per point are used in the near-edge and extended region, respectively, for NaF. After correcting for the elastic-scattering energy of each analyzer, the spectra at each q are normalized to absolute units by a simultaneous fit to the RSFMS-calculated atomic background outside the near-edge region and a Pearson function over a wide energy range for removal of the valence Compton background.[34,38] For NaCl, we obtain 2.1×10^3 counts above a background of 1.1×10^4 counts at the Na K edge at q=4.3 Å^{-1} and 9.8×10^3 counts above a background of 5.9×10^4 counts at the Na K edge at q=11.1 Å^{-1}. For NaF, we obtain 1.7×10^4 counts above a background of 4.2×10^4 counts at the Na K edge at q=4.3 Å^{-1} and 7.8×10^4 counts above a background of 1.5×10^5 counts at the Na K edge at q=11.1 Å^{-1}. Data binning and q averaging follow methods previously described.[18,37,39] We estimate a 20% systematic uncertainty in the normalization to absolute units for each q, due to the combination of theoretical uncertainties in the calculation of the q-dependent atomic background[9] and the *ad hoc* use of the Pearson form for the tail of the valence Compton profile.[34,38]

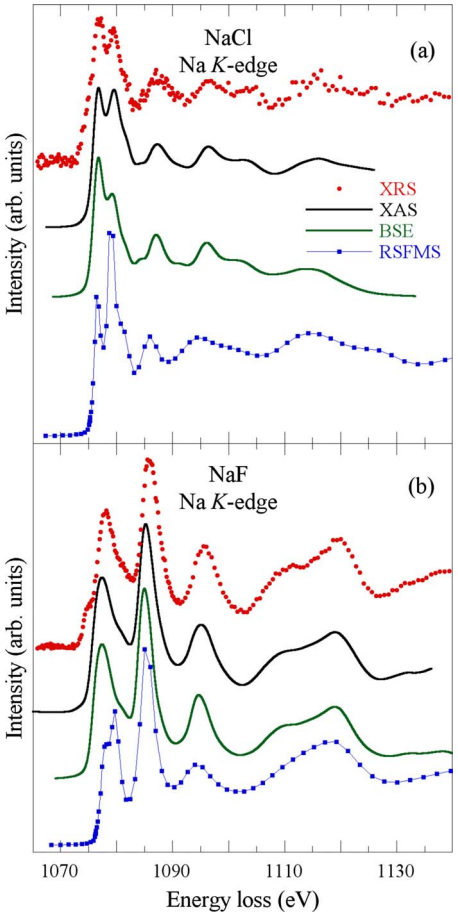

FIG. 1. (Color online) Na K-edge extended structure for (a) NaCl and (b) NaF. XRS data (top) are represented by filled circles. Poisson errors for the XRS data are approximately four times the size of the symbols in (a) and equal to the size of the symbols in (b). XAS data from Kikas *et al.* (Ref. 22), broadened to the present experiment's energy resolution to aid comparison, are presented as the second curve from the top (solid line). The third curve from the top shows the BSE calculation. The bottom curve in each panel shows the RSFMS calculation. All curves are normalized to the height of the first major peak and offset for clarity.

IV. RESULTS AND DISCUSSION

In Figs. 1(a) and 1(b), we show the Na 1*s* extended XRS spectra for NaCl and NaF, respectively. The XRS spectra are weighted averages of the individual XRS spectra for all fourteen analyzer-detector pairs (q=4.3–11.1 Å^{-1}). Also shown in each panel are the XAS results of Kikas *et al.*,[22,23] broadened to match the energy resolution of the present measurements (second curve from the top), and calculations using BSE and RSFMS methods (third and fourth curves from the top, respectively). All curves are normalized to the height of the first major peak and offset for clarity. Except for a strong q-dependent feature in the pre-edge region, which we will discuss in more detail below, the feature-by-feature agreement between the XRS, XAS, BSE, and RSFMS spectra is quite good. In the very near-edge region, peak heights are extremely sensitive to the strength of the electron-core hole interaction and band-structure effects. Hence the discrepan-

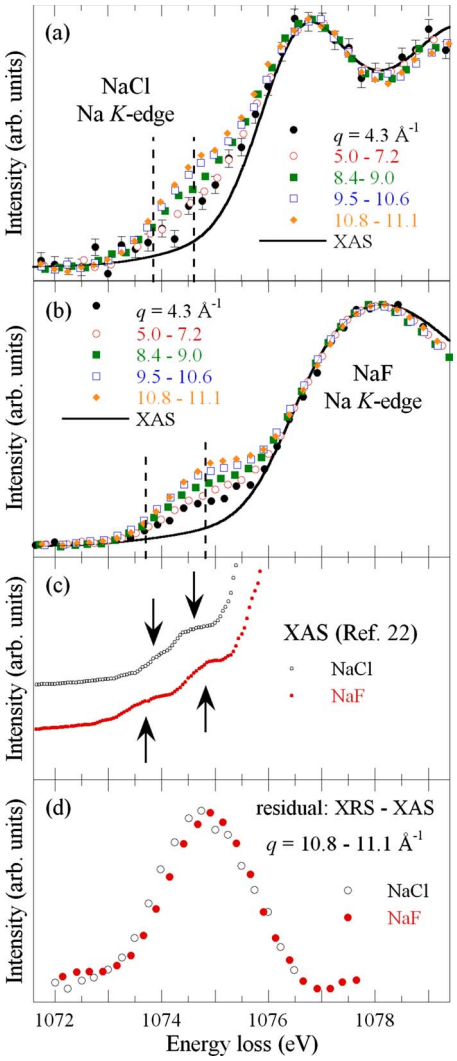

FIG. 2. (Color online) Na *K*-edge near-edge structure for (a) NaCl and (b) NaF. XRS data are presented in order of increasing q as labeled in the legend. The ranges of q correspond to qa=0.32, 0.38–0.54, 0.64–0.68, 0.71–0.80, and 0.82–0.84, respectively. All undisplayed error bars for the XRS data are of the size of the symbols or smaller. XAS data (solid line) in (a) and (b) are from Kikas *et al.* (Ref. 22), broadened to match the present experiment's energy resolution to aid comparison. Panel (c) shows an enlargement of the unbroadened XAS data over a limited energy range. The arrows indicate the position of the small pre-edge features. The vertical dashed lines in panels (a) and (b) are at the same energies as the respective arrows. Panel (d) shows an *ad hoc* measure of the nondipole XRS signal, obtained by subtracting the broadened XAS spectra from the highest-momentum-transfer XRS curves. See the text for discussion.

cies between calculated and measured spectra seen in Fig. 1 are understandable.

In Fig. 2, we focus on the very near-edge structure at the Na *K* edge of NaCl and NaF, respectively. The XRS spectra shown in Figs. 2(a) and 2(b) are the result of binning individual spectra into the five indicated ranges in q. The broadened XAS spectra of Kikas *et al.*[22,23] provide dipole-limited reference spectra. For ease of presentation, the XRS and broadened XAS results are normalized by the intensity of the

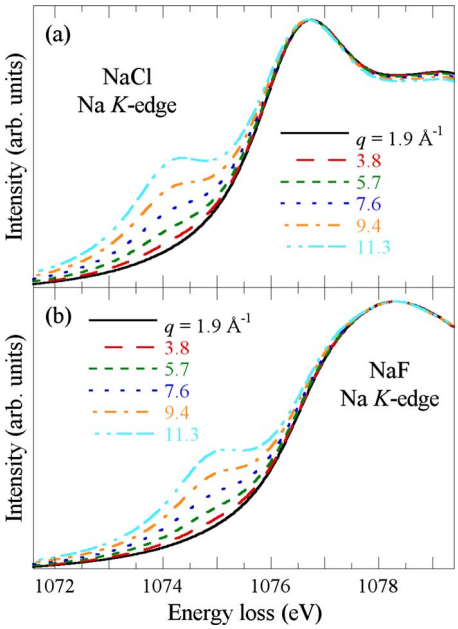

FIG. 3. (Color online) BSE calculations of the Na *K*-edge near-edge structure for (a) NaCl and (b) NaF. The calculated spectra are presented in order of increasing q as labeled in the legend.

first major peak. For both NaCl and NaF, the XRS spectra show an increase in the magnitude of the pre-edge feature relative to the first major peak with increasing q. In Fig. 2(c) we show an enlarged view of the unbroadened XAS results.[22,23] Note the clear presence of two pre-edge features for NaF and the less well-resolved corresponding peaks in the NaCl spectrum. The arrows indicate estimated peak locations and the dashed lines in Figs. 2(a) and 2(b) are at the corresponding energies. For both NaCl and NaF, the strong q-dependent feature occurs at energies much more consistent with the higher-energy pre-edge features than the lower-energy features. This is illustrated in Fig. 2(d), where we show an *ad hoc* characterization of the nondipole XRS contribution in this energy region by subtracting the broadened XAS results from the high-q XRS spectra. In Fig. 3, we show q-dependent BSE calculations for the Na *K* edge for both materials. These calculations show qualitative agreement with the XRS spectra; there is no evidence for two pre-edge features and the magnitude of the observed pre-edge feature increases with increasing q.

These results demonstrate the presence of dipole-forbidden final states in the pre-edge region for both NaCl and NaF. We now address whether the orbital angular momentum of these excitations can be determined from the q dependence of the XRS intensity,[2,3,18,20,21] before discussing possible explanations for the weak or zero contribution to the XRS signal of the lower-energy excitons observed in the XAS spectra.

It is clear from Eq. (3) that two criteria must be satisfied in order for a sharp spectral feature to appear in an XRS spectrum: there must be a sharp feature in at least one component of the l DOS, and the associated weighting factor $(2l+1)|M_l(q,\omega)|^2$ must have significant amplitude in the experimentally accessible range of q and physically relevant

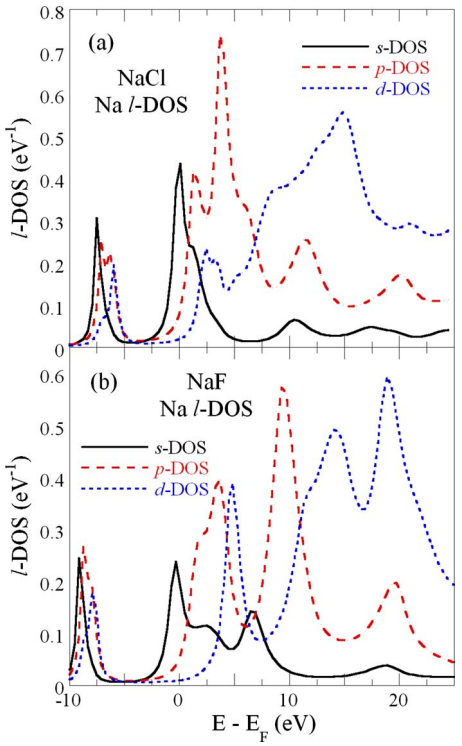

FIG. 4. (Color online) RSFMS calculations of the Na *l* DOS for (a) NaCl and (b) NaF.

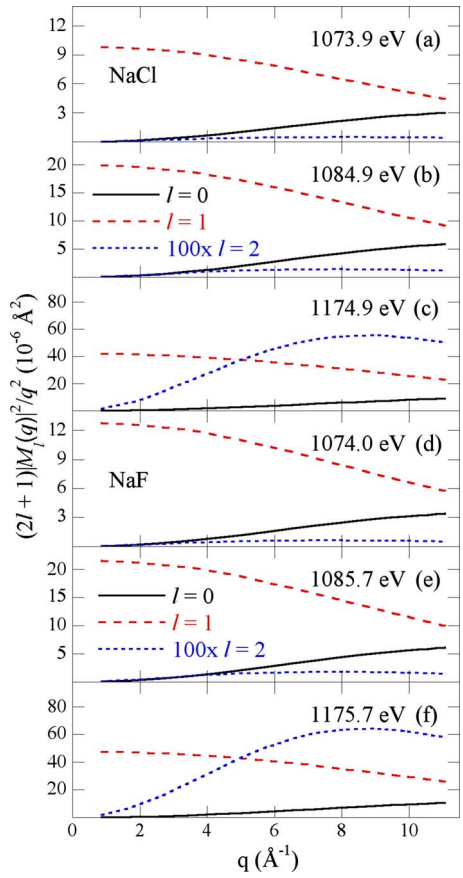

FIG. 5. (Color online) The calculated *l*-DOS weighting factors $(2l+1)|M_l(q,\omega)|^2$, scaled by q^2, based on Na 1*s* initial states for NaCl (a,b,c) and NaF (d,e,f) at the indicated energies. Note that the $l=2$ curve has been increased by a factor of 100 in all panels.

range of ω. In Figs. 4(a) and 4(b), we show the RSFMS calculations for Na *l* DOS for NaCl and NaF, respectively. In both NaCl and NaF, there is significant weight in the *s* DOS peaked just below or at the ground-state Fermi energy E_F consistent with the assignment of an *s*-type bound state. Note that there is no weight in the *d* DOS for either compound until well above (approximately 1.5 and 3.0 eV for NaCl and NaF, respectively) the nominal absorption edge at the midpoint in the rise of the *p* DOS ($E-E_F$=0.6 and 0.9 eV for NaCl and NaF, respectively).

In Fig. 5, we show the calculated $(2l+1)|M_l(q,\omega)|^2$ coefficients appearing in Eq. (3), scaled by q^2, as a function of q for each compound at three selected energies. The energies are chosen, respectively, to be very close to E_F, safely into the near-edge regime and somewhat into the extended regime. At all energies and all experimentally accessible q, the coupling to *p*-type final states is largest but the coupling to *s*-type final states is also significant, especially at high q. In all panels of the figure the $l=2$ curves have been multiplied by 100; there is essentially zero coupling to *d*-type final states from the 1*s* initial state at all energy losses and q. As a consequence, XRS from the Na 1*s* initial state will not be sensitive to *d*-type final states, should any exist. We return to this issue shortly.

On the basis of the qualitative aspects of calculated *l* DOS (Fig. 4) and coefficients for Eq. (3) (Fig. 5), the observed q-dependent pre-edge features in NaCl and NaF must be *s* type. This may also be tested quantitatively. Given that these excitations are relatively localized in energy, it is natural to calculate the q dependence of their generalized oscillator strength

$$\mathrm{GOS}(q) = \frac{2m}{q^2}\int d\omega\omega S(q,\omega), \tag{6}$$

where the integral is performed over the relevant energy range.[40] In Fig. 6 we show the measured and calculated GOS(q). The experimental measure for GOS(q) is determined by fitting $S(q,\omega)$ to two Gaussian peaks in the immediate near-edge region. Due to uncertainty in the absolute energy scale, we fixed the energy difference between the centers of the two Gaussians to 2.47 eV for NaCl and 3.37 eV for NaF but included the center of the main peak as a variable in the fit. We then evaluated Eq. (6) for the lower-energy Gaussian peak (corresponding to the pre-edge feature). The error bars are dominated by the experimental uncertainty due to absolute normalization of $S(q,\omega)$. The BSE GOS(q) is calculated from the *s*-to-*s* transition contribution to $\varepsilon_2(q,\omega)$. In atomic units, $S(q,\omega)$ is related to $\varepsilon_2(q,\omega)$ by the expression

$$S(q,\omega) \approx \frac{\Omega_C q^2}{4\pi^2}\varepsilon_2(q,\omega), \tag{7}$$

where Ω_C is the unit-cell volume. The RSFMS GOS(q) is determined from the contribution to $S(q,\omega)$ from the *s*-type DOS above the band gap but below the nominal absorption

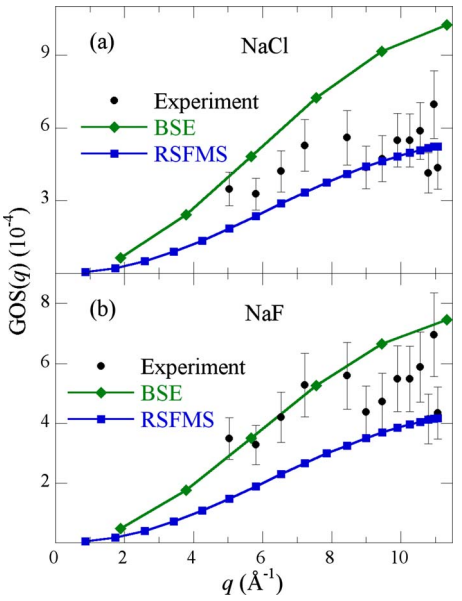

FIG. 6. (Color online) GOS in the bound region for the theoretical *s*-type contribution calculated by BSE (solid triangles) and RSFMS (solid squares) and measured by XRS (Fig. 2) as a function of momentum transfer for (a) NaCl and (b) NaF. See the text for details.

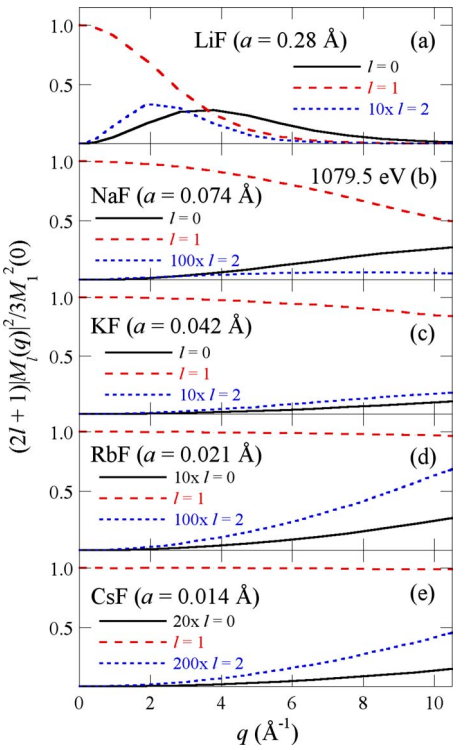

FIG. 7. (Color online) Calculated $(2l+1)|M_l(q,\omega)|^2$ for the 1*s* initial states of the alkali atom in LiF, NaF, KF, RbF, and CsF, normalized by the $l=1$ value in the dipole limit ($q=0$). The parameter *a* is the mean radius of the 1*s* initial state for the alkali atom. For each calculation, the photoelectron final-state energy was chosen to be 5 eV above the Fermi energy; the value of the energy is included in panel (b) for comparison to panels (d)–(f) of Fig. 5. Note the large multiplying factors needed to bring the $l=2$ terms onto the scale of the figure. As a consequence, transitions to *d*-type final states from the 1*s* initial state are effectively unobservable in the near-edge region, even at large *q*.

edge (midpoint in rise of the *p* DOS, see Fig. 4). The agreement between the theory and experiment provides additional support that the respective pre-edge features in NaCl and NaF are *s*-type excitons.

The weak sensitivity to *d*-type final states for *q*-dependent XRS from 1*s* initial states deserves further comment. In Figs. 7 and 8, we compare calculated $(2l+1)|M_l(q,\omega)|^2$ coefficients for the 1*s* and 2*s* initial states of several alkali fluorides. All calculations are performed at 5 eV past the Fermi energy; this choice is safely within the near-edge regime and away from instabilities due to the inexact determination of the Fermi energy. The results on each panel are normalized by the natural scale set by the *p*-type channel at $q=0$, i.e., the dipole limit. While it is generically the case that the $l=2$ contribution to the XRS will be small for the 1*s* initial state (Fig. 7), this is not true for 2*s* initial states (Fig. 8), whose greater spatial extent allows for significant overlap with *d*-type orbitals. While we are unfamiliar with any XRS measurement for a 2*s* initial state for an alkali-metal atom, a significant amplitude has been observed for $2s \rightarrow \varepsilon d$ transitions in *q*-dependent XRS measurements of Al and Mg.[30] These results may be helpful in planning future *q*-dependent XRS studies. In cases for which XRS is insensitive to $l \geq 2$ final states, a small number of momentum transfers is sufficient for experimental determination of the *s* and *p* DOS. However, a large number of momentum transfers is useful to over specify the system of equations[18] and is necessary for decomposition of the *l* DOS when a greater number of orbital angular momenta contribute to the XRS spectra.

Before concluding, we discuss possible explanations for the occurrence of two excitons in the XAS results in NaCl and NaF for the 1*s* core hole. The results presented here exclude the suggestion that both NaF features are *d* type.[23] While the weak spin-flip scattering in NRIXS would indeed make our measurements insensitive to a $^3S_1$-triplet final state, as has been considered for the lower-energy feature,[23] the same would be true for XAS measurements because of the conservation of total spin by the dipole operator. Hence, it is difficult to explain the lower-energy features as being second bulk dipole-forbidden excitons.

However, it is interesting to consider whether these features may be surface core excitons. Surface core excitons were first observed in GaAs by Lapeyre and Anderson,[41] and have subsequently been observed in several alkali halides.[42–44] The surface exciton always appears at lower energy than the bulk exciton, by an amount as large as 1.3 eV for the Li 1*s* initial state in LiCl.[43] The details of the XAS experiments, where evaporated 10-nm-thick films were studied with 40° angle of incidence of the x-ray beam[22,23] may give some sensitivity to surface excitations despite the nominally bulklike penetration length for radiation at the Na *K* edge. Given that the two XAS pre-edge features for each material appear with similar intensities, any surface contributions may need to be at least weakly dipole allowed. A combined study of the photoelectron and absorption spectra for the Na 2*p* initial states of NaCl and NaF finds evidence

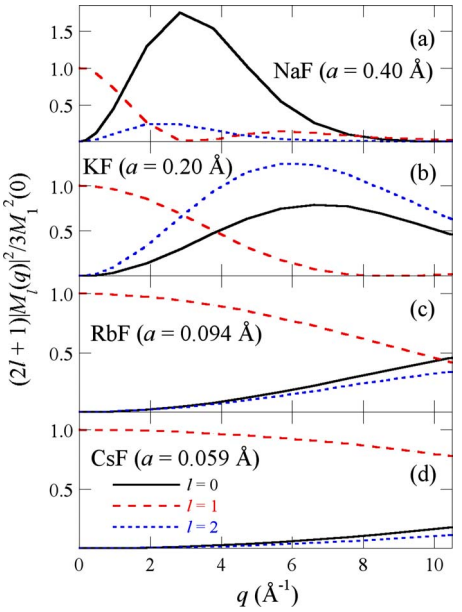

FIG. 8. (Color online) Calculated $(2l+1)|M_l(q,\omega)|^2$ for the 2*s* initial states of the alkali atom in NaF, KF, RbF, and CsF, normalized by the $l=1$ value in the dipole limit ($q=0$). The parameter a is the mean radius of the 2*s* initial state for the alkali atom. For each calculation, the photoelectron final-state energy was chosen to be 5 eV above the Fermi energy. Unlike the calculations for the 1*s* initial states (Fig. 7), transitions to *d*-type final states may be observed at experimentally accessible values of q.

for two excitonic states in each material. For NaCl the behavior of the lower-energy feature indicates that it is a surface exciton. However, the behavior of the lower-energy feature for NaF is not consistent with a surface exciton, and is instead proposed to be a second, bulklike exciton.[44] The different photoelectron-hole interactions for the 1*s* and 2*p* core holes may be relevant. New XAS measurements of the Na 1*s* core excitons in both materials, taken as a function of the angle to the surface of both the incident radiation and the polarization vector would be beneficial to help resolve this dilemma. Given the significant penetration length of both materials at the Na *K* edge, transmission-mode XAS studies are also possible and would give a useful, unambiguous bulk characterization.

Finally, it is fair to ask whether the differences in the XAS and XRS results may be due to an inherent limitation of XRS; the cross section for this process is very small and consequently the samples experience long exposures in intense beams. All alkali halides can show beam-damage effects and in the present case the samples showed significant blackening in only a very thin layer at the surface, presumably due to ozone damage from residual air in the sample chamber. However, there are several issues which make beam damage an unlikely explanation for the absence of the lower-energy exciton in the XRS spectra. The strongest evidence against beam damage is the otherwise strong agreement between XRS, XAS, and theory from the edge to 40 eV past the edge. Additional support comes from the good qualitative and quantitative agreement between XRS and theory as regards the character and q dependence of the observed exciton for each material. Most generally, any beam-damage effect which sufficiently disturbs the local atomic structure so as to remove one distinct pre-edge resonance is necessarily *bulklike* and hence it is difficult to reconcile such damage with the absence of strong influence on so many other features which are also highly sensitive to local atomic structure. Hence, while we cannot experimentally exclude that beam-damage effects may remove the second exciton from the XRS spectra, we believe it to be very unlikely.

V. CONCLUSIONS

We have presented new q-dependent measurements of the Na 1*s* contribution to the NRIXS from NaCl and NaF. These measurements, together with new calculations using the real-space full multiple-scattering method and the Bethe-Salpeter equation, determine that the higher-energy core excitons identified in previous XAS and resonant Auger studies are predominantly *s* type for each material. However, the lower-energy core excitons seen in the previous studies are absent in the NRIXS measurements. The small probability of $1s \rightarrow \varepsilon d$ transitions and small amplitude for spin-flip scattering are discussed and excluded as explanations for a second bulk core exciton that is not probed by NRIXS. We propose that the lower-energy features are surface core excitons and suggest further measurements to test this hypothesis. We further discuss the implications of the small probability of $1s \rightarrow \varepsilon d$ transitions for future q-dependent measurements.

ACKNOWLEDGMENTS

This research was supported by the U.S. Department of Energy, Basic Energy Sciences, Office of Science, under Contracts No. DE-FGE03-97ER45628 and No. W-31-109-ENG-38, Office of Naval Research under Grant No. N00014-05-1-0843, and the Summer Research Institute program at the Pacific Northwest National Laboratory. The operation of Sector 20 PNC-CAT/XOR is supported by the U.S. Department of Energy, Basic Energy Sciences, Office of Science, under Contract No. DE-FG03-97ER45629, the University of Washington, and grants from the Natural Sciences and Engineering Research Council of Canada. Use of the Advanced Photon Source was supported by the U.S. Department of Energy, Basic Energy Sciences, Office of Science, under Contract No. DE-AC02-06CH11357. We thank Arvo Kikas, Micah Prange, Joshua Kas, and John Rehr for useful discussions.

*Corresponding author. seidler@phys.washington.edu

[1] S. Albrecht, L. Reining, R. Del Sole, and G. Onida, Phys. Rev. Lett. **80**, 4510 (1998); M. Rohlfing and S. G. Louie, Phys. Rev. B **62**, 4927 (2000).

[2] Y. J. Feng, G. T. Seidler, J. O. Cross, A. T. Macrander, and J. J. Rehr, Phys. Rev. B **69**, 125402 (2004); K. Hamalainen, S. Galambosi, J. A. Soininen, E. L. Shirley, J. P. Rueff, and A. Shukla, *ibid.* **65**, 155111 (2002).

[3] Y. J. Feng, J. A. Soininen, A. L. Ankudinov, J. O. Cross, G. T. Seidler, A. T. Macrander, J. J. Rehr, and E. L. Shirley, Phys. Rev. B **77**, 165202 (2008).

[4] A. Kivimaki, B. Kempgens, K. Maier, H. M. Koppe, M. N. Piancastelli, M. Neeb, and A. M. Bradshaw, Phys. Rev. Lett. **79**, 998 (1997).

[5] H. P. Hjalmarson, H. Buttner, and J. D. Dow, Phys. Rev. B **24**, 6010 (1981); R. S. Knox, *Theory of Excitons* (Academic Press, New York, 1963).

[6] A. L. Ankudinov, A. I. Nesvizhskii, and J. J. Rehr, Phys. Rev. B **67**, 115120 (2003); E. L. Shirley, J. Electron Spectrosc. Relat. Phenom. **144-147**, 1187 (2005); M. Rohlfing and S. G. Louie, Phys. Rev. Lett. **80**, 3320 (1998); **81**, 2312 (1998); L. X. Benedict, E. L. Shirley, and R. B. Bohn, Phys. Rev. B **57**, R9385 (1998); Phys. Rev. Lett. **80**, 4514 (1998); L. X. Benedict and E. L. Shirley, Phys. Rev. B **59**, 5441 (1999); E. L. Shirley, J. A. Soininen, and J. J. Rehr, Phys. Scr., T **T115**, 31 (2005); J. J. Rehr, J. A. Soininen, and E. L. Shirley, *ibid.* **T115**, 207 (2005); G. Strinati, Phys. Rev. Lett. **49**, 1519 (1982); Phys. Rev. B **29**, 5718 (1984); W. Olovsson, I. Tanaka, T. Mizoguchi, P. Puschnig, and C. Ambrosch-Draxl, *ibid.* **79**, 041102 (2009); A. L. Ankudinov, Y. Takimoto, and J. J. Rehr, *ibid.* **71**, 165110 (2005); M. Taillefumier, D. Cabaret, A.-M. Flank, and F. Mauri, *ibid.* **66**, 195107 (2002); O. Wessely, O. Eriksson, and M. I. Katsnelson, *ibid.* **73**, 075402 (2006); O. Wessely, M. I. Katsnelson, and O. Eriksson, Phys. Rev. Lett. **94**, 167401 (2005); G. Onida, L. Reining, and A. Rubio, Rev. Mod. Phys. **74**, 601 (2002); J. A. Soininen and E. L. Shirley, Phys. Rev. B **61**, 16423 (2000); F. M. F. de Groot, Inorg. Chim. Acta **361**, 850 (2008); P. Krüger and C. R. Natoli, Phys. Rev. B **70**, 245120 (2004); A. Kotani, J. Electron Spectrosc. Relat. Phenom. **100**, 75 (1999); F. M. F. de Groot, Z. W. Hu, M. F. Lopez, G. Kaindl, F. Guillot, and M. Tronc, J. Chem. Phys. **101**, 6570 (1994); M. Abbate, R. Potze, G. A. Sawatzky, and A. Fujimori, Phys. Rev. B **49**, 7210 (1994); D. Prendergast and G. Galli, Phys. Rev. Lett. **96**, 215502 (2006); L. Triguero, L. G. M. Pettersson, and H. Agren, Phys. Rev. B **58**, 8097 (1998); M. Cavalleri, H. Ogasawara, L. G. M. Pettersson, and A. Nilsson, Chem. Phys. Lett. **364**, 363 (2002); C. Kolczewski, R. Püttner, O. Plashkevych, H. Ågren, V. Staemmler, M. Martins, G. Snell, A. S. Schlachter, M. Sant'Anna, G. Kaindl, and L. G. M. Pettersson, J. Chem. Phys. **115**, 6426 (2001); H. Ostrom, H. Ogasawara, L. A. Naslund, K. Andersson, L. G. M. Pettersson, and A. Nilsson, *ibid.* **127**, 10 (2007).

[7] E. L. Shirley, J. Electron Spectrosc. Relat. Phenom. **136**, 77 (2004).

[8] E. L. Shirley, Ultramicroscopy **106**, 986 (2006).

[9] J. A. Soininen, A. L. Ankudinov, and J. J. Rehr, Phys. Rev. B **72**, 045136 (2005).

[10] J. A. Soininen, J. J. Rehr, and E. L. Shirley, J. Phys.: Condens. Matter **15**, 2573 (2003).

[11] J. A. Soininen, K. Hamalainen, W. A. Caliebe, C. C. Kao, and E. L. Shirley, J. Phys.: Condens. Matter **13**, 8039 (2001); J. A. Soininen and E. L. Shirley, Phys. Rev. B **64**, 165112 (2001).

[12] Y. Mizuno and Y. Ohmura, J. Phys. Soc. Jpn. **22**, 445 (1967); K. Tohji and Y. Udagawa, Phys. Rev. B **36**, 9410 (1987); K. Tohji and Y. Udagawa, *ibid.* **39**, 7590 (1989); Y. Udagawa, N. Watanabe, and H. Hayashi, J. Phys. IV **7**, 347 (1997); N. Watanabe, H. Hayashi, Y. Udagawa, K. Takeshita, and H. Kawata, Appl. Phys. Lett. **69**, 1370 (1996); W. Schulke, K. J. Gabriel, A. Berthold, and H. Schulteschrepping, Solid State Commun. **79**, 657 (1991).

[13] P. Wernet, D. Nordlund, U. Bergmann, M. Cavalleri, M. Odelius, H. Ogasawara, L. Å. Näslund, T. K. Hirsch, L. Ojamäe, P. Glatzel, L. G. M. Pettersson, and A. Nilsson, Science **304**, 995 (2004); M. Balasubramanian, C. S. Johnson, J. O. Cross, G. T. Seidler, T. T. Fister, E. A. Stern, C. Hamner, and S. O. Mariager, Appl. Phys. Lett. **91**, 031904 (2007); U. Bergmann, A. DiCicco, P. Wernet, E. Principi, P. Glatzel, and A. Nilsson, J. Chem. Phys. **127**, 174504 (2007); U. Bergmann, P. Glatzel, and S. P. Cramer, Microchem. J. **71**, 221 (2002); M. Krisch and F. Sette, Surf. Rev. Lett. **9**, 969 (2002).

[14] S. K. Lee, P. J. Eng, H. K. Mao, Y. Meng, M. Newville, M. Y. Hu, and J. F. Shu, Nature Mater. **4**, 851 (2005); W. L. Mao, Ho-kwang Mao, Peter J. Eng, Thomas P. Trainor, Matthew Newville, Chi-chang Kao, Dion L. Heinz, Jinfu Shu, Yue Meng, and Russell J. Hemley, Science **302**, 425 (2003).

[15] H. Sternemann, J. A. Soininen, C. Sternemann, K. Hamalainen, and M. Tolan, Phys. Rev. B **75**, 075118 (2007).

[16] H. Sternemann, C. Sternemann, J. S. Tse, S. Desgreniers, Y. Q. Cai, G. Vankó, N. Hiraoka, A. Schacht, J. A. Soininen, and M. Tolan, Phys. Rev. B **75**, 245102 (2007).

[17] M. H. Krisch, F. Sette, C. Masciovecchio, and R. Verbeni, Phys. Rev. Lett. **78**, 2843 (1997).

[18] T. T. Fister, F. D. Vila, G. T. Seidler, L. Svec, J. C. Linehan, and J. O. Cross, J. Am. Chem. Soc. **130**, 925 (2008).

[19] S. Galambosi, M. Knaapila, J. A. Soininen, K. Nygard, S. Huotari, F. Galbrecht, U. Scherf, A. P. Monkman, and K. Hamalainen, Macromolecules **39**, 9261 (2006).

[20] S. Galambosi, J. A. Soininen, K. Nygard, S. Huotari, and K. Hamalainen, Phys. Rev. B **76**, 195112 (2007).

[21] J. A. Soininen, A. Mattila, J. J. Rehr, S. Galambosi, and K. Hamalainen, J. Phys.: Condens. Matter **18**, 7327 (2006).

[22] A. Kikas, E. Nommiste, R. Ruus, A. Saar, and I. Martinson, Surf. Rev. Lett. **9**, 1303 (2002).

[23] A. Kikas, E. Nõmmiste, R. Ruus, A. Saar, and I. Martinson, Phys. Rev. B **64**, 235120 (2001).

[24] T. Murata, T. Matsukawa, and S. Naoe, Solid State Commun. **66**, 787 (1988).

[25] U. Bergmann, O. C. Mullins, and S. P. Cramer, Anal. Chem. **72**, 2609 (2000); U. Bergmann, D. Nordlund, P. Wernet, M. Odelius, L. G. M. Pettersson, and A. Nilsson, Phys. Rev. B **76**, 024202 (2007); U. Bergmann, P. Wernet, P. Glatzel, M. Cavalleri, L. G. M. Pettersson, A. Nilsson, and S. P. Cramer, *ibid.* **66**, 092107 (2002); D. T. Bowron, M. H. Krisch, A. C. Barnes, J. L. Finney, A. Kaprolat, and M. Lorenzen, *ibid.* **62**, R9223 (2000); C. Sternemann, J. A. Soininen, S. Huotari, G. Vanko, M. Volmer, R. A. Secco, J. S. Tse, and M. Tolan, *ibid.* **72**, 035104 (2005).

[26] P. Wernet, D. Testemale, J. L. Hazemann, R. Argoud, P. Glatzel, L. G. M. Pettersson, A. Nilsson, and U. Bergmann, J. Chem. Phys. **123**, 154503 (2005).

[27] Y. Q. Cai, H.-K. Mao, P. C. Chow, J. S. Tse, Y. Ma, S. Patchkovskii, J. F. Shu, V. Struzhkin, R. J. Hemley, H. Ishii, C. C.

Chen, I. Jarrige, C. T. Chen, S. R. Shieh, E. P. Huang, and C. C. Kao, Phys. Rev. Lett. **94**, 025502 (2005); H. Fukui, S. Huotari, D. Andrault, and T. Kawamoto, J. Chem. Phys. **127**, 134502 (2007); J. F. Lin, Hiroshi Fukui, David Prendergast, Takuo Okuchi, Yong Q. Cai, Nozomu Hiraoka, Choong-Shik Yoo, Andrea Trave, Peter Eng, Michael Y. Hu, and Paul Chow, Phys. Rev. B **75**, 012201 (2007); W. L. Mao, H. K. Mao, Y. Meng, P. J. Eng, M. Y. Hu, P. Chow, Y. Q. Cai, J. F. Shu, and R. J. Hemley, Science **314**, 636 (2006); Y. Meng, Ho-kwang Mao, Peter J. Eng, Thomas P. Trainor, Matthew Newville, Michael Y. Hu, Chichang Kao, Jinfu Shu, Daniel Hausermann, and Russell J. Hemley, Nature Mater. **3**, 111 (2004).

[28] S. K. Lee, P. J. Eng, H. K. Mao, Y. Meng, and J. Shu, Phys. Rev. Lett. **98**, 105502 (2007).

[29] A. Sakko, M. Hakala, J. A. Soininen, and K. Hamalainen, Phys. Rev. B **76**, 205115 (2007); M. W. Haverkort, A. Tanaka, L. H. Tjeng, and G. A. Sawatzky, Phys. Rev. Lett. **99**, 257401 (2007).

[30] T. T. Fister, G. T. Seidler, C. Hamner, J. O. Cross, J. A. Soininen, and J. J. Rehr, Phys. Rev. B **74**, 214117 (2006).

[31] R. A. Gordon, G. T. Seidler, T. T. Fister, M. W. Haverkort, G. A. Sawatzky, A. Tanaka, and T. K. Sham, EPL **81**, 26004 (2008); A. Mattila, J. A. Soininen, S. Galambosi, S. Huotari, G. Vanko, N. D. Zhigadlo, J. Karpinski, and K. Hamalainen, Phys. Rev. Lett. **94**, 247003 (2005); C. Sternemann, M. Volmer, J. A. Soininen, H. Nagasawa, M. Paulus, H. Enkisch, G. Schmidt, M. Tolan, and W. Schulke, Phys. Rev. B **68**, 035111 (2003).

[32] T. T. Fister, G. T. Seidler, E. L. Shirley, F. D. Vila, J. J. Rehr, K. P. Nagle, J. C. Linehan, and J. O. Cross, J. Chem. Phys. **129**, 044702 (2008).

[33] R. D. Leapman, P. Rez, and D. F. Mayers, J. Chem. Phys. **72**, 1232 (1980); S. T. Manson, Phys. Rev. A **6**, 1013 (1972).

[34] T. T. Fister, Ph.D. dissertation, University of Washington, 2007.

[35] A. L. Ankudinov, B. Ravel, J. J. Rehr, and S. D. Conradson, Phys. Rev. B **58**, 7565 (1998); J. J. Rehr and R. C. Albers, Rev. Mod. Phys. **72**, 621 (2000).

[36] J. H. Burnett, Z. H. Levine, E. L. Shirley, and J. H. Bruning, J. Microlithogr., Microfabr., Microsyst. **1**, 213 (2002).

[37] T. T. Fister, G. T. Seidler, L. Wharton, A. R. Battle, T. B. Ellis, J. O. Cross, A. T. Macrander, W. T. Elam, T. A. Tyson, and Q. Qian, Rev. Sci. Instrum. **77**, 063901 (2006).

[38] H. Sternemann, C. Sternemann, G. T. Seidler, T. T. Fister, A. Sakko, and M. Tolan, J. Synchrotron Radiat. **15**, 162 (2008).

[39] T. T. Fister, K. P. Nagle, F. D. Vila, G. T. Seidler, C. Hamner, J. O. Cross, and J. J. Rehr, Phys. Rev. B **79**, 174117 (2009).

[40] M. Inokuti, Rev. Mod. Phys. **43**, 297 (1971).

[41] G. J. Lapeyre and J. Anderson, Phys. Rev. Lett. **35**, 117 (1975).

[42] O. Aita, K. Ichikawa, and K. Tsutsumi, Phys. Rev. B **38**, 10079 (1988); M. Kamada, O. Aita, K. Ichikawa, and K. Tsutsumi, *ibid.* **36**, 4962 (1987); T. Mabuchi, H. Toda, and H. Yamanaka, J. Phys. Soc. Jpn. **62**, 246 (1993).

[43] K. Ichikawa, O. Aita, M. Kamada, and K. Tsutsumi, Phys. Rev. B **43**, 5063 (1991).

[44] K. Ichikawa, O. Aita, and K. Tsutsumi, Phys. Rev. B **39**, 1307 (1989).